Engineering Fracture Mechanics, 1971, Vol. 3, pp. 435–451. Pergamon Press. Printed in Great Britain

PLASTIC INTENSITY FACTORS FOR CRACKED PLATES†

PETER D. HILTON and JOHN W. HUTCHINSON
Harvard University, Cambridge, Mass. 02138, U.S.A.

Abstract—An elastic-plastic analysis is performed for two problems relevant to fracture mechanics: a semi-infinite body with an edge crack in a far out-of-plane shearing field and an infinite plate under plane stress conditions containing a finite line crack in a remote tensile field. Amplitudes of the dominant singularity in the plastic region at the crack tip, the plastic stress and strain intensity factors, are calculated for applied stress levels approaching the yield stress. A technique is developed for using the dominant singular solution in conjunction with the finite element method to make accurate calculations for the near-tip fields. Additionally, a comparative study of deformation theory with flow theory is performed for cracks in an anti-plane shear field. Elastic fracture mechanics is extended to high levels of applied stress for which the plastic zone is no longer small compared to the crack length by relating the critical stress for fracture initiation to the plastic intensity factors.

INTRODUCTION

AN ELASTIC-plastic analysis of plates of hardening material containing cracks will be carried out. This analysis is then employed to extend classical fracture mechanics to the case when the plastic zone about the crack tip can no longer be considered small. Work pertinent to this area of fracture mechanics has been reviewed by McClintock and Irwin[1] and very recently by Rice[2].

Initiation of crack growth depends on the stress and strain fields in the immediate vicinity of the crack tip. For the cases considered in the present study, cracks in remote anti-plane shear and tensile fields, these near-tip solutions are known except for their amplitudes, the plastic stress and strain intensity factors which relate the behavior at the crack tip to the geometry and applied stress. In the small scale yielding range, when the plastic zone about the crack tip is small in comparison with the crack length, the plastic intensity factors can be related directly to the elastic stress intensity factor. Results of this type, which will be further discussed, are due to Hult and McClintock[3], Neuber[4] and Rice[5] for the anti-plane shear case and to Rice and Rosengren[6] and Hutchinson[7, 8] for the tensile case. At higher values of applied stress, in what will be referred to as the large scale yielding range, the plastic zone is no longer small compared to the crack length and the elastic stress intensity factor is no longer relevant without some modification.

Use of plastic intensity factors is in no way restricted by the extent of the plastic zone; and thus the concept of a critical value of the plastic stress or strain intensity factor can be introduced and employed in much the same way as the elastic stress intensity factor is used in classical fracture mechanics. A numerical procedure is developed here which combines details of the dominant singularity in the plastic region with the finite element technique for accurate computation of the plastic intensity factors. Standard numerical techniques which have been applied to these crack problems with no special treatment for the singularity at the crack tip fail to give accurate solutions about the tip, the region of prime interest.

†Presented at the Third National Symposium on Fracture Mechanics, Lehigh University, Bethlehem, Pa., August 25–27, 1969.

The problem of a semi-infinite body with an edge crack subjected to a far out-of-plane shear field is used to illustrate the techniques developed. Accuracy estimates for this problem for the case of a deformation theory of plasticity are established through comparisons with the results which Rice[5] obtained with a different technique. Further, the calculations are repeated with an incremental theory to study the discrepancies between the predictions of deformation theory and those based on flow theory. The major contribution of this work is the results which have been obtained for a finite line crack in an infinite sheet under plane stress conditions subjected to a tensile field.

PLASTIC STRESS AND STRAIN INTENSITY FACTORS

The dominant singular term of the elastic solution in the neighborhood of a crack tip is written as

$$\sigma_{ij} = \frac{K_{el}}{\sqrt{2\pi r}} \tilde{\sigma}_{ij}(\theta) \tag{1}$$

where (r, θ) are polar coordinates centered at the tip.† A collection of elastic solutions to crack problems for a variety of geometries and loading conditions is given in the review paper by Paris and Sih[9]. For all loadings and geometries such that the stress fields are symmetric (or antisymmetric), the circumferential variation of the stress field, $\tilde{\sigma}_{ij}(\theta)$, is independent of additional features of both the geometry and the boundary conditions of the particular problem considered. Only the amplitude K_{el}, commonly called the stress intensity factor, varies from problem to problem. Fracture initiation takes place, for a given set of conditions, when the amplitude of the stress field at the crack tip reaches a critical value. This approach presumes that the plastic zone is sufficiently small so that (1) represents the stress field accurately in the neighborhood of the crack tip outside the plastic zone.

It is now standard procednre to experimentally determine the value of the stress intensity factor at which fracture initiates and to apply the results to initial fracture prediction for other configurations. There are a number of necessarily restrictive conditions which must be placed on this technique, and details such as conditions approaching plane stress and plane strain must be differentiated as discussed in [10].

A simple example which illustrates elastic fracture mechanics is that of an infinite

$$\sigma_{ij} = \frac{K_{el}}{\sqrt{2\pi r}} \tilde{\sigma}_{ij}(\theta) \tag{1}$$

where (r, θ) are polar coordinates centered at the tip.† A collection of elastic solutions to crack problems for a variety of geometries and loading conditions is given in the review paper by Paris and Sih[9]. For all loadings and geometries such that the stress fields are symmetric (or antisymmetric), the circumferential variation of the stress field, $\tilde{\sigma}_{ij}(\theta)$, is independent of additional features of both the geometry and the boundary conditions of the particular problem considered. Only the amplitude K_{el}, commonly called the stress intensity factor, varies from problem to problem. Fracture initiation takes place, for a given set of conditions, when the amplitude of the stress field at the crack tip reaches a critical value. This approach presumes that the plastic zone is sufficiently small so that (1) represents the stress field accurately in the neighborhood of the crack tip outside the plastic zone.

It is now standard procednre to experimentally determine the value of the stress intensity factor at which fracture initiates and to apply the results to initial fracture prediction for other configurations. There are a number of necessarily restrictive conditions which must be placed on this technique, and details such as conditions approaching plane stress and plane strain must be differentiated as discussed in [10].

A simple example which illustrates elastic fracture mechanics is that of an infinite

As discussed in the Introduction, the dominant singularity in the plastic zone for hardening materials will be exploited to extend elastic fracture mechanics, and the plastic stress (or strain) intensity factor associated with the dominant term for the near-tip fields will be used in a manner analogous to the elastic stress intensity factor to correlate fracture initiation results.

A small strain formulation of plasticity is used as the basis for the present studies. The tensile stress–strain relations

$$\epsilon = \begin{matrix} \sigma; & \sigma \leqslant 1 \\ \sigma^n; & \sigma > 1 \end{matrix} \tag{3}$$

are chosen to model the tensile elastic-plastic behavior of the material where the material coefficient is n.

For the present discussion a total deformation theory of plasticity is employed. Plastic deformation is assumed to be independent of the hydrostatic component of stress, σ_{kk}, and completely determined by the first invariant of the stress deviator $s_{ij} = \sigma_{ij} - \frac{1}{3}\sigma_{kk}\delta_{ij}$. This invariant, the 'effective stress' σ_e, is defined by $\sigma_e^2 = \frac{3}{2}s_{ij}s_{ij}$. For simple tension $\sigma_e = \sigma$ and the Mises yield condition is $\sigma_e = 1$. The generalized stress–strain relationship which reduces to (3) for simple tension is

$$s_{ij} = \begin{matrix} e_{ij}/(1+\nu); & \sigma_e \leqslant 1 \\ [e_e/(1+\nu)]^{(1-n)/n}\, e_{ij}/(1+\nu); & \sigma_e > 1 \end{matrix} \tag{4}$$

valid only for anti-plan shear and/or $\nu = 1/2$

where ν is Poisson's ratio, the strain deviator is $e_{ij} = \epsilon_{ij} - \frac{1}{3}\epsilon_{pp}\delta_{ij}$ and the effective strain e_e is defined by $e_e^2 = \frac{3}{2}e_{ij}e_{ij}$. In the subsequent formulation it will be assumed that no unloading occurs for the monotonic loading histories considered in this paper. This necessitates an *a posteriori* check of the solution to assure that this assumption has not been violated.

As in the elastic analysis, the dominant singular term of the asymptotic expansion at the crack tip can be written as an intensity factor multiplying a function which is independent of geometry and boundary conditions. For plane stress, plane strain, and anti-plane shear the dominant fields associated with a 'power hardening material' can be written in the following form

$$\begin{aligned} \sigma_{ij} &= K_\sigma r^{-1/(n+1)}\, \tilde{\sigma}_{ij}(\theta) \\ \epsilon_{ij} &= K_\epsilon r^{-n/(n+1)}\, \tilde{\epsilon}_{ij}(\theta) \end{aligned} \tag{5}$$

where $K_\epsilon = (K_\sigma)^n$ and where the dimensionless functions of θ, $\tilde{\sigma}_{ij}$ and $\tilde{\epsilon}_{ij}$, are detailed for plane stress and plane strain in [8].†

In the region at the crack tip dominated by the singularity solution (5) the deformation is proportional, that is, the relative magnitudes of the stress components do not change with increasing applied load. For this reason, (5) is valid for flow theory as well as deformation theory; however, in general, the amplitudes will differ depending on which theory is employed.

†Unlike in [8], here r is the distance from the crack tip and has not been normalized by the crack length $2a$.

It must be emphasized that the concept of an ~~elastic~~ plastic strain intensity factor associated with a dominant singularity is tied to hardening materials. The distribution of strain at the tip of a crack in a perfectly plastic material is no longer in one to one correspondence with the stress distribution and, in most cases, $\tilde{\epsilon}_{ij}(\theta)$ will depend on the applied stress. Alternate measures of the crack tip deformation are possible in this limiting case, but they will not be dwelt on here.

Asymptotic expressions relating the plastic intensity factors to the elastic stress intensity factor, valid for small scale yielding, can be obtained using the methods outlined in [6, 7]. These results are of the form

$$K_\sigma = c_n(K_{el}/\sqrt{\pi})^{2/n+1}, \quad K_\epsilon = (K_\sigma)^n \tag{6}$$

and values of the coefficients c_n, which depend on the hardening coefficient, are given for a number of cases for both plane stress and plane strain in [8]. For an infinite plate containing a line crack of length $2a$, K_σ and K_ϵ can be rewritten as

$$K_\sigma = c_n(\sigma^\infty)^{2/n+1}a^{1/n+1}, K_\epsilon = (c_n)^n(\sigma^\infty)^{2n/n+1}a^{n/n+1}. \tag{7}$$

In the large scale yielding range (7) no longer holds and in its place are expressions of the form

$$K_\sigma = f(\sigma^\infty)a^{1/n+1}, K_\epsilon = f^n a^{n/n+1} \tag{8}$$

where f will be calculated up to values of $\sigma^\infty = 0{\cdot}9$ for the problems investigated in this paper.

In direct analog to elastic fracture mechanics, critical values for the plastic stress and strain intensity factors associated with fracture initiation, $K_\sigma{}^c$ and $K_\epsilon{}^c = (K_\sigma{}^c)^n$, are introduced. In the small scale yielding range, when K_σ, K_ϵ and K_{el} are directly related by (6), the predictions based on the plastic intensity factors are identical to those based on the elastic stress intensity factor. When large scale yielding occurs, K_σ and K_{el} are no longer directly related, independent of the crack length, and it will be necessary to use (8) to modify the elastic predictions.

ELASTIC-PLASTIC ANALYSIS OF CRACKED BODIES IN ANTI-PLANE SHEAR

The equations governing the anti-plane shear case are simpler in form than those for in-plane problems so that it is convenient to use this problem as a model to exhibit the techniques developed in the present work. Further, the numerical results can be compared to those that Rice [5] obtained with a different technique.

Consider an infinite body containing a finite straight crack subjected to a remote, out-of-plane shearing field. From symmetry considerations, this is the same problem as that of a semi-infinite body containing an edge crack (Fig. 1). Let w represent the displacement normal to the plane of the plate. The only non-zero strains are $\gamma_{xz} = w_{,x}$ and $\gamma_{yz} = w_{,y}$.† The dominant singular solution for a power hardening material of the form given by (4) has been derived by Neuber [4] and Rice [5]. With polar coordinates

†In this section only, $(\bar{\tau}_{xz}, \bar{\tau}_{yz}, K_\sigma) = (\bar{\tau}_{xz}, \bar{\tau}_{yz}, \bar{K}_\sigma)/\bar{\tau}_Y$ where τ_Y is the yield stress in shear and $(\epsilon_{xz}, \epsilon_{yz}, K_\epsilon) = (\bar{\gamma}_{xz}, \bar{\gamma}_{yz}, K_\epsilon)/\bar{\gamma}_Y$ where $\bar{\gamma}_Y \equiv \bar{\tau}_Y/G$ and $w = \bar{w}/\bar{\gamma}_Y$.

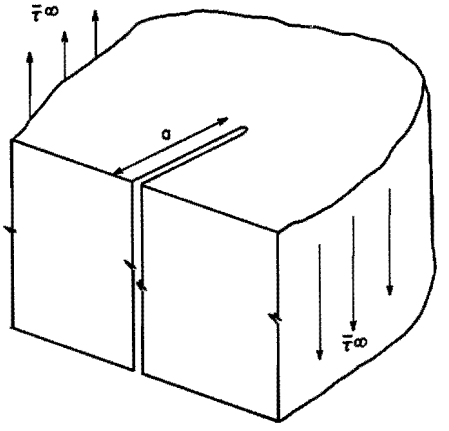

Fig. 1(a). A semi-infinite body with an edge crack in a remote anti-plane shear field.

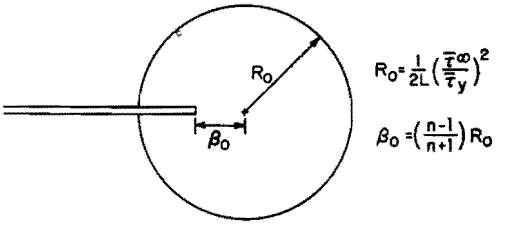

Fig. 1(b). The elastic-plastic boundary for small scale yielding in anti-plane shear.

(r, θ) centered at the crack tip, this solution can be reduced to the form

$$\begin{Bmatrix}\tau_{xz}\\ \tau_{yz}\end{Bmatrix} = K_\sigma \left[\frac{h(\theta)}{r}\right]^{1/(n+1)} \begin{Bmatrix}-\sin\rho\\ \cos\rho\end{Bmatrix}$$

$$\begin{Bmatrix}\gamma_{xz}\\ \gamma_{yz}\end{Bmatrix} = K_\epsilon \left[\frac{h(\theta)}{r}\right]^{n/(n+1)} \begin{Bmatrix}-\sin\rho\\ \cos\rho\end{Bmatrix} \tag{9}$$

$$w = K_\epsilon \left[\frac{h(\theta)}{r}\right]^{-1/(n+1)} \sin\rho$$

where

$$2\rho = \theta - \arcsin\left[\left(\frac{n-1}{n+1}\right)\sin\theta\right], \quad h(\theta) = \frac{\sin 2\rho}{2\sin\theta} \quad \text{and} \quad K_\epsilon = (K_\sigma)^n.$$

For small scale yielding, the character of the entire field is exceptionally simple as has been discussed in [5]. The plastic zone bounded by a circle of radius $\tau^{\infty 2}a/2$ with its center shifted a distance $\tau^{\infty 2}a/2(n-1/n+1)$ ahead of the crack tip is shown in Fig. 1(b). The plastic stress intensity factor is given by

$$K_\sigma = \tau^{\infty 2/(n+1)}\, a^{1/(n+1)}. \tag{10}$$

Moreover, (9) is the full solution everywhere in the plastic zone. The plastic deformation is exactly proportional and this solution is also a solution to J_2 flow theory.

Attention is now directed to the large scale yielding problem for which the shape of the plastic zone becomes non-circular and (10) for K_σ no longer holds. A numerical procedure is developed to connect, or match, the field at the crack tip which is governed by the dominant singularity to the uniform stress field ($\tau_{xz} = 0$, $\tau_{yz} = \tau^\infty$) far from the crack. A finite element technique is specialized to this purpose. The variational principle of minimum potential energy for deformation theory plasticity forms the basis for this method. A modified potential energy functional is introduced next which remains finite for all admissible displacement fields and can, therefore, be applied to the infinite domain under consideration.

Let Γ_R be a circular arc centered at the intersection of the axes and of sufficient radius, R, so that the plastic region is contained within it as shown in Fig. 2. Designate the

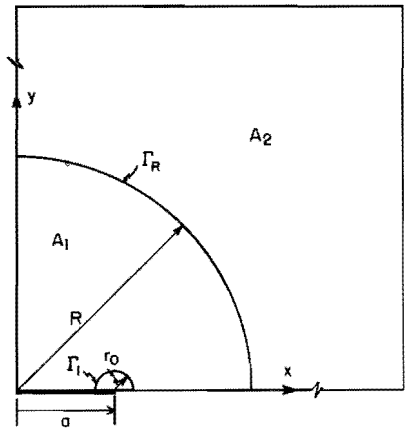

Fig. 2. The division of the quarter plane into two regions associated with the modified potential energy functional.

region outside Γ_R as region A_2, the region inside Γ_R as A_1. In A_2, the displacements are written for the general case as the sum of u_i^0 and $\tilde{u}_i$, where u_i^0 is chosen in such a way that $\tilde{u}_i = (u_i - u_i^0)$ is of order $(1/r)$ for large R.

The modified potential energy functional is

$$MPE = \int_{A_1} SED(u_i)\mathrm{d}A + \int_{A_2} SED(\tilde{u}_i)\mathrm{d}A - \int_{\Gamma_R} \sigma_{ij}^0 n_j \tilde{u}_i \mathrm{d}s \tag{11}$$

where $SED(u_i) = \int_0^{\epsilon_{ij}} \sigma_{ij}\mathrm{d}\epsilon_{ij}$, $SED(u_i) = \frac{1}{2}\tilde{\sigma}_{ij}\tilde{\epsilon}_{ij}$, n_j is the outward unit normal to Γ_R and σ_{ij}^0 are the stresses derived from u_i^0. It can be shown that the functional MPE for a monotonically hardening material is minimized by the exact solution among all admissible fields u_i in A_1 and $\tilde{u}_i$ in the infinite domain A_2. In the present application, $w^0 = \tau^\infty y$ which corresponds to the uniform stress state approached far from the crack, and $\sigma_{ij}^0 n_j \tilde{u}_i = \tau^\infty \tilde{w} \sin\theta$ on Γ_R.

In A_2, the solution is expressible in terms of an analytic function of the complex variable z, $\phi(z)$, where

$$w = \mathrm{Real}[\phi(z)] \quad \text{and} \quad \tau_{xz} - i\tau_{yz} = \phi'(z).$$

The symmetry conditions are used to write the Laurent series for $\phi(z)$ about the origin as

$$\phi(z) = -i\tau^{\infty} z + \sum_{m=1}^{\infty} i a_m z^{-2m+1} = \phi_0 + \tilde{\phi} \quad \text{for} \quad |z| \geq R \tag{12}$$

where $\phi_0 = -i\tau^{\infty} z$ and the a_m are real. The series is convergent on and outside of Γ_R. On Γ_R,

$$w(R, \theta) = R\tau^{\infty} \sin\theta + \sum_{m=1}^{\infty} a_m R^{-2m+1} \sin(2m-1)\theta. \tag{13}$$

The coefficients a_m are related to the displacement field along Γ_R by

$$a_m = -R^2 \tau^{\infty} \beta_{1m} + \frac{4}{\pi} R^{2m-1} \int_0^{\pi/2} w(R, \theta) \sin(2m-1)\theta \, d\theta \tag{14}$$

where $\beta_{1m} = 1$ for $m = 1$ and $\beta_{1m} = 0$ for $m \neq 1$. In what follows, symmetry is exploited and integrations are performed over only the first quadrant of the x, y plane. The contribution from A_2 to MPE is

$$\int_{A_2} SED(\tilde{w}) dA = \frac{1}{2} \int_R^{\infty} r dr \int_0^{\pi/2} d\theta (\tilde{\phi}' \bar{\tilde{\phi}}') = \frac{\pi}{8} \sum_{m=1}^{\infty} a_m^2 (2m-1) R^{-4m+2}.$$

Attention is now focused on the immediate vicinity of the crack tip. Consider a circular arc, Γ_1, centered at the tip and contained in the fully plastic region. If r_0, the radius to Γ_1, is taken sufficiently small, then the dominant term of the expansion (9), which is asymptotically correct at the crack tip, is a good representation to the full solution on and within Γ_1. The strain energy of the region within Γ_1, calculated from the dominant singular solution is

$$SE = \frac{n}{n+1} \int_0^{r_0} r dr \int_0^{\pi} d\theta (\tau^{n+1}) = K_{\epsilon}^{(n+1)/n} \frac{n}{n+1} \frac{r_0}{2} \int_0^{\pi} \frac{\sin 2\rho}{\sin\theta} d\theta \equiv K_{\epsilon}^{(n+1)/n} S_n$$

and the displacement field on Γ_1 is given by

$$w = K_{\epsilon} \left[\frac{h(\theta)}{r_0} \right]^{-1/(n+1)} \sin\rho \equiv K_{\epsilon} W(\theta).$$

The final form of the modified potential energy functional can be written as

$$MPE = K_{\epsilon}^{(n+1)/n} S_n + \int_{A_1^*} SED(w) dA + \frac{\pi}{8} \sum_1^{\infty} a_m^2 (2m-1) R^{-4m+2} - \int_{\Gamma_R} \tau^{\infty} \sin\theta \, \tilde{w}(R, \theta) R d\theta \tag{15}$$

where A_1^* is the area between Γ_1 and Γ_R. The displacement field along Γ_1 is now known except for its amplitude K_{ϵ} which will be determined through the minimization of MPE.

A finite element technique is employed to provide a representation of the solution in the region between Γ_1 and Γ_R. This region is divided into a triangular grid pattern. Over each element, the displacement field is approximated by a general linear function; thus the strain components in each element are constant[13]. The strain energy of an element is expressed in terms of the displacements at the three nodes of the triangular element. For a typical element, the strain energy is

$$SE = D \sum_{i,j=1}^{3} B_{ij} w_i w_j$$

where B_{ij} is a symmetric matrix whose elements depend only on the triangle geometry and D is a nonlinear coefficient related to the element stiffness and given by $D = 1$ if the element is elastic and, if not, by

$$D = (\gamma_{xz}^2 + \gamma_{yz}^2)^{1-n/2n}.$$

The Laurent series for the solution in A_2 is terminated at a finite number of terms arbitrarily chosen to equal the number of nodal points along Γ_R. The coefficients a_m are calculated in terms of the displacements at the nodes along Γ_R using (14).

The above procedure results in a discretization of the modified potential energy functional which depends on the plastic strain intensity factor K_ϵ and the nodal displacements w_i. Equilibrium equations associated with the minimization of MPE with respect to each of these parameters are given by

$$\frac{\partial MPE(K_\epsilon, w_i)}{\partial K_\epsilon} = 0, \quad \frac{\partial MPE(K_\epsilon, w_i)}{\partial w_j} = 0 \quad j = 1, M \tag{16}$$

where M is the total number of nodal points in the grid pattern. Equations (16) are nonlinear algebraic in form and an iterative procedure is used to solve them. A choice of initial values for the coefficients D of the stiffness matrix for each element and for the stiffness parameter, $K_\epsilon^{(1-n)/n}$, for the inner core region bounded by Γ_1 renders the system of equations linear in the nodal deflections and K_ϵ. This large system of equations is solved and the coefficients D and $K_\epsilon^{(1-n)/n}$ are recalculated. The iterative process is continued until convergence is attained.

The accuracy of these calculations depends on the number and distribution of elements and on the radius r_0 chosen for the inner boundary. A grid pattern consisting of 546 elements with the inside radius r_0 equal to two percent of the crack length was chosen. Eleven node points are taken along the half-circular arcs near the crack tip. The resulting procedure for a given value of τ^∞ converged within six iterations for all cases considered with a reasonable set of initial guesses. The strain invariant for each element increased with increasing values of the loading parameter. Thus unloading did not occur and its exclusion in the formation of the stress-strain relations is justified. A comparison with the results by Rice[5] indicated that the accuracy of the technique for a material with high strain hardening capacity was quite good and the results were never more than two percent in error for $n = 10/3$. However, when the strain hardening capacity diminished as in the case of $n = 10$, values for the plastic strain intensity factor were as much às five percent low for large values of the applied stress.

The deviation of the plastic strain intensity factor from the small scale yielding value as given by (10) is shown in Fig. 3(a). Specifically, the ratio $\lambda(\tau^\infty) \equiv K_\epsilon/(K_\epsilon)_{s.s.y.}$, which

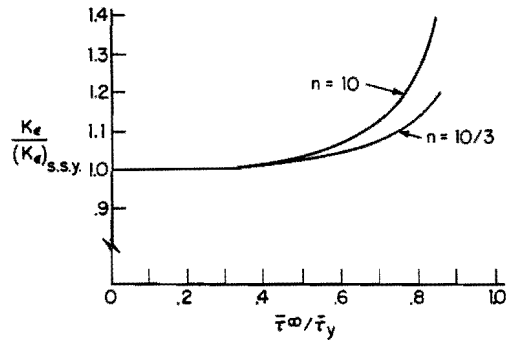

Fig. 3(a). The plastic strain intensity factor as a function of the applied stress for anti-plane shear.

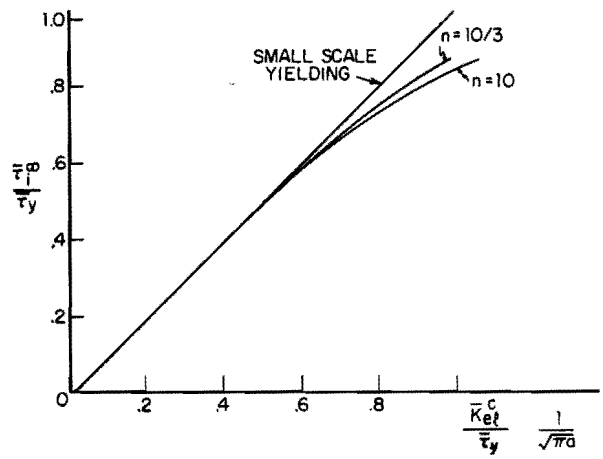

Fig. 3(b). The critical initiation stress for large scale yielding, anti-plane shear.

by (7) and (8) is independent of the crack length, is plotted against $\tau^\infty \equiv \bar{\tau}^\infty/\bar{\tau}_Y$. These results are now employed in conjunction with the fracture criterion, that K_ϵ reach the critical value $K_\epsilon{}^c$ when the crack starts to extend, to predict the critical initiation stress in the large scale yielding range. Using the critical elastic stress intensity factor and the identity (6) in the small scale yielding range, an implicit equation for τ_i^∞ results:

$$\tau_i^\infty = \frac{K^c_{el}}{[\lambda(\tau_i^\infty)]^{n+1/2n}} \cdot \frac{1}{\sqrt{\pi a}}. \tag{17}$$

In this form it is clear by comparison with (2) that $K^c_{el}/[\lambda(\tau_i^\infty)]^{n+1/2n}$ can be regarded as the modified 'elastic' stress intensity factor. Plots of $\bar{\tau}_i^\infty/\bar{\tau}_Y$ vs. $\bar{K}^c_{el}/\bar{\tau}_Y\sqrt{\pi a}$ are given in Fig. 3(b); and thus, deviations from the 45° line at roughly half the yield stress indicate a departure from the predictions of elastic fracture mechanics.

The plastic intensity factors for the anti-plane shear problem treated above were recalculated using an incremental theory of plasticity. The same uniaxial stress–strain curve was used in conjunction with J_2 flow theory. As has already been noted, the form of the dominant singularity given by (5) and (9) will still hold for this incremental

theory but the amplitude out of the small scale yielding range will, in general, differ from the predictions of deformation theory.

Most of the aspects of the incremental theory calculation are similar to the method discussed in the foregoing. A modified strain rate functional, specialized to the incremental problem, is again used together with the embedded singularity. In this calculation, however, the load is increased in small steps and a sequence of linear incremental problems is solved. Now, increments of the intensity factor K_ϵ, as well as the nodal displacements w_i, are solved. Since the small scale yielding solution is correct for J_2 flow theory as well as deformation theory, it is used to 'start' the incremental solution at a sufficiently low value of the applied stress. Accuracy checks were made in several ways. First, the effect of varying the load increments was determined, and second, this same incremental procedure was applied to the deformation theory problem for which a comparison with known results was possible. The plastic strain intensity factors calculated on this basis for flow theory for the cases $n = 10/3$ and $n = 10$ up to the value $\tau^\infty = 0{\cdot}9$ were only very slightly below the corresponding predictions of deformation theory and were within the accuracy of the numerical method.

To further demonstrate the versatility of the techniques developed in this section, the linear-elasticity problem was also solved with the same grid pattern. The calculated value for the stress intensity factor was well within one percent of the known value. Thus, the method described for combining the knowledge of the character of the singular solution with a finite element technique may turn out to be a useful technique for the determination of elastic intensity factors associated with complicated geometries. Other work along these lines is already underway[11], including a fairly sophisticated analysis of this type of procedure[12].

CRACKED PLATES IN TENSILE FIELDS

The techniques which have been developed for the anti-plane shear problem are applicable to the tensile case with only minor revision. In this section both the small and large scale yielding problem for an infinite plate under plane stress conditions containing a finite line crack in a far tensile field will be treated. Deformation theory is employed.

The extended Michell theorem[14] is exploited to permit consideration of an incompressible material. This considerably simplifies the stress-strain relations in the plastic region. The theorem states that for problems with tractions specified on all boundaries, the stress field is independent of Poisson's ratio. Note that the features of interest, namely, the plastic stress intensity factor and the plastic strain intensity factor, which is related to it by $K_\epsilon = (K_\sigma)^n$, as well as the elastic-plastic boundary, are independent of Poisson's ratio for plane stress conditions.

Small scale yielding analysis

Here our primary interests are to obtain an accurate description of the elastic-plastic boundary and to determine the accuracy that this type of calculation, which will later be employed for the general problem, gives for the plastic intensity factor. The small scale yielding problem is the asymptotic problem posed for the case in which the plastic zone is very small in comparison with the crack length, $2a$, so that it is embedded in the elastic field dominated by the singular elastic solution. Mathematically, the problem treated is a plate with a semi-infinite crack in a far stress field which is the elastic

singular solution, i.e.

$$\begin{Bmatrix} \bar{\sigma}_{rr} \\ \bar{\sigma}_{r\theta} \\ \bar{\sigma}_{\theta\theta} \end{Bmatrix} = \frac{K_{el}}{\sqrt{2\pi r}} \begin{Bmatrix} 5/4\cos\theta/2 - 1/4\cos 3\theta/2 \\ 1/4\sin\theta/2 + 1/4\sin 3\theta/2 \\ 3/4\cos\theta/2 + 1/4\cos 3\theta/2 \end{Bmatrix} \tag{18}$$

where $\bar{K}_{el} = \bar{\sigma}^{\infty}\sqrt{\pi a}$.

The solution asymptotically close to the crack tip is the dominant singular solution whose form is given in (5). The circumferential variation of the fields ($\tilde{\sigma}_{ij}(\theta)$ and $\tilde{\epsilon}_{ij}(\theta)$) associated with the singular solution are reproduced from Ref. [8] in Fig. 4. For the

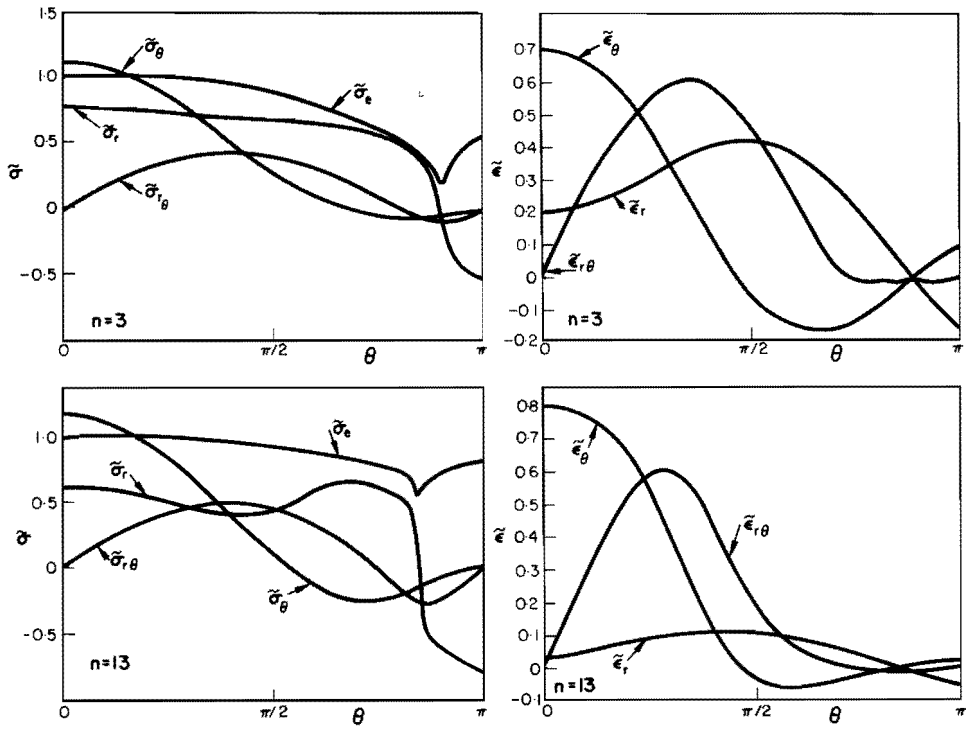

Fig. 4. θ-Variation of stresses and strains at the tip of a tensile crack for plane stress (from [7]).

small scale yielding problem, the plastic strain intensity factor is given by (7). The values for c_n given in [8] which will be used here for comparison purposes are

$$c_n = \begin{cases} 0{\cdot}949 & n = 3 \\ 1{\cdot}004 & n = 9. \end{cases} \tag{19}$$

The following non-dimensionalization collapses the set of solutions corresponding to different values of $\sigma^{-\infty}$ into one set of similar solutions:

$$(\hat{u}, \hat{v}) = \frac{1}{a}\left(\frac{\bar{\sigma}_Y}{\bar{\sigma}^\infty}\right)^2 \left(\frac{\bar{u}}{\bar{\epsilon}_Y}, \frac{\bar{v}}{\bar{\epsilon}_Y}\right), \qquad (\hat{x}, \hat{y}) = \frac{1}{a}\left(\frac{\bar{\sigma}_Y}{\bar{\sigma}^\infty}\right)^2 (x, y)$$

$$\hat{\sigma}_{ij} = \frac{\bar{\sigma}_{ij}}{\bar{\sigma}_Y}, \qquad \hat{\epsilon}_{ij} = \frac{\bar{\epsilon}_{ij}}{\bar{\epsilon}_Y} \tag{20}$$

$$\hat{K}_\sigma = \frac{\bar{K}_\sigma}{\bar{\sigma}_Y}[(\bar{\sigma}_Y/\bar{\sigma}^\infty)^2/a]^{1/n+1}, \qquad \hat{K}_\epsilon = \frac{\bar{K}_\epsilon}{\bar{\epsilon}_Y}[(\bar{\sigma}_Y/\bar{\sigma}^\infty)^2/a]^{n/n+1}$$

where u, x, σ_{ij}, and ϵ_{ij} satisfy the same equations as $\bar{u}$, x, $\bar{\sigma}_{ij}$, and $\bar{\epsilon}_{ij}$ respectively. The far stress field with this non-dimensionalization is the same (18) with $\bar{K}_{\rm II}/\sqrt{2\pi r}$ replaced by $1/\sqrt{2\hat{r}}$. The non-dimensionalized plastic intensity factors are $\hat{K}_\sigma = c_n$ and $\hat{K}_\epsilon = (c_n)^n$. This non-dimensionalization is only for the small scale yielding problem and will be used exclusively throughout this section. For convenience the '^' symbol will be omitted henceforth.

As in the anti-plane shear case, the plane is divided into two regions associated with the modified potential energy functional. Denote as Γ_{R_s} a circular arc centered at the crack tip and of sufficient radius R_s so that the plastic zone is contained within it. In region A_2, outside Γ_{R_s}, the solution is written in terms of the Muskhelishvili[15] functions ϕ and ψ where (with $\nu = \frac{1}{2}$)

$$\begin{aligned} \sigma_y - \sigma_x + 2i\sigma_{xy} &= 2(\bar{z}\phi'' + \psi') \\ \sigma_x + \sigma_y &= 2(\phi' + \bar{\phi}') \\ u + iv &= 5/2\phi - 3/2(z\bar{\phi}' + \bar{\psi}). \end{aligned} \tag{21}$$

The expansions for ϕ and ψ which satisfy the stress-free condition along the crack and symmetry are

$$\begin{aligned} \phi &= z^{1/2}/\sqrt{2} + \sum_{m=1}^{\infty} a_m z^{-m+1/2} = \phi_0 + \tilde{\phi} \\ \psi &= z^{1/2}/2\sqrt{2} + \sum_{m=1}^{\infty} (m + 1/2) a_m z^{-m+1/2} = \psi_0 + \tilde{\psi} \end{aligned} \tag{22}$$

where each a_m is real, and $\phi_0 = z^{1/2}/\sqrt{2}$ and $\psi_0 = z^{1/2}/2\sqrt{2}$ are the terms which correspond to the far field of the dominant singularity of the elastic solution. The unknown coefficients a_m can be expressed in terms of the displacements along Γ_{R_s}, $u(R, \theta)$, etc. as

$$a_m = R_s^{m-1/2} \frac{2}{5\pi} \int_0^\pi [(u + iv) - (u_0 + iv_0)]\, e^{i(m-1/2)\theta}\, d\theta.$$

The contribution from A_2 to the modified potential energy functional is found to be

$$SE_2(\tilde{u}) = \frac{\pi}{2} \sum_{m=1}^{\infty} (-m + 1/2)[(1 + 3(m + 1/2)^2) a_m^2 r^{-2m+1} - 3(m + 3/2)(-m + 5/2) a_m a_{m+2} r^{-2m-1}].$$

A circular arc Γ_1 of radius r_0 is centered at the crack tip and the dominant singular solution described previously is used to obtain the fields on and within Γ_1. The values

for the circumferential variation of the displacements along Γ_1 were obtained from the calculations made in [7]. This information is used, just as in the anti-plane shear case, to determine the contribution of the inner core to the modified potential energy.

The region between Γ_1 and Γ_{R_s} is divided into a node pattern by a series of concentric circular arcs and a set of radial lines. The resulting quadrangles are each divided into two triangles, and in this way the finite element technique with constant strain, triangular elements is used to connect the region between Γ_1 and Γ_{R_s}. This leads to a set of nonlinear algebraic equations for K_ϵ and the nodal displacements whose solution is carried out in the same way as it was for the anti-plane shear problem.

Computations were performed for two values of the hardening coefficient, $n = 3$ and 9. In each case the inside radius $\hat{r}_0$ was taken to be 0·03 and the grid pattern consisted of 1080 elements with 21 nodes on each half circular arc. For $n = 3$, this resulted in a numerical value for the plastic strain intensity factor which was 3 per cent above the known value (19). When the material hardening capacity was decreased to $n = 9$, the calculated value was 2 per cent higher. Plots of the elastic-plastic boundaries in non-dimensional similarity coordinates $(\hat{x}, \hat{y})$ are presented in Fig. 5. Also included is a

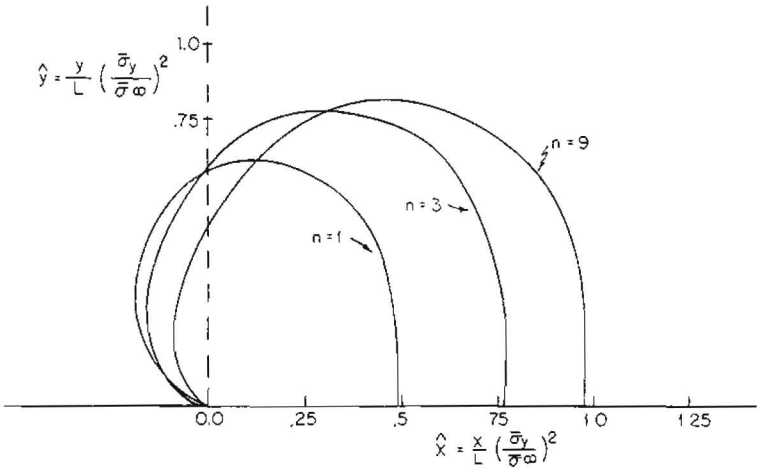

Fig. 5. Elastic-plastic boundaries for small scale yielding in a tensile field.

calculated value was 2 per cent higher. Plots of the elastic-plastic boundaries in non-dimensional similarity coordinates $(\hat{x}, \hat{y})$ are presented in Fig. 5. Also included is a

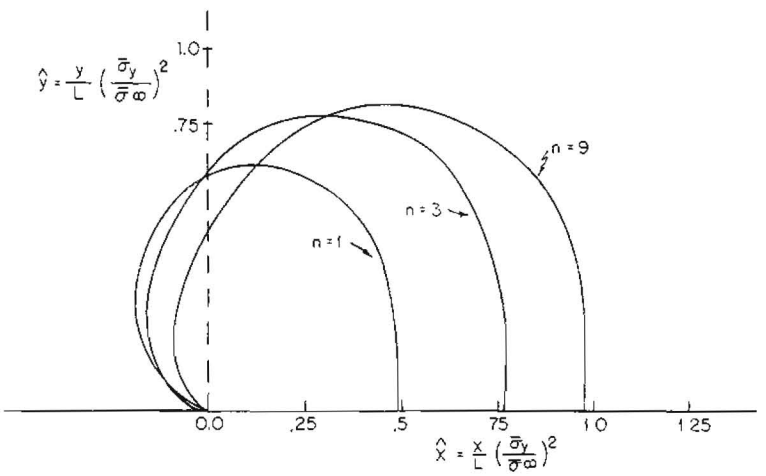

Fig. 5. Elastic-plastic boundaries for small scale yielding in a tensile field.

sions for $\tilde{\phi}$ and $\tilde{\psi}$ which satisfy the symmetry conditions about both axes for $|z| \geq R$, are

$$\tilde{\phi} = \sum_{m=1}^{\infty} a_{2m-1} z^{-2m+1}$$
$$\tilde{\psi} = \sum_{m=1}^{\infty} b_{2m-1} z^{-2m+1}$$

where a_m and b_m are real. Outside Γ_R, $\phi = \phi_0 + \tilde{\phi}$ and $\psi = \psi_0 + \tilde{\psi}$. The coefficients a_m and b_m are related to the displacements along Γ_R by

$$a_m = \frac{3R^2\sigma^\infty}{10}\beta_{1m} + \frac{4R^m}{5\pi}\int_0^{\pi/2} (u+iv)\, e^{im\theta}\, d\theta \qquad m = 1, 3, 5\ldots$$

$$b_1 = \frac{R^2\sigma^\infty}{6} - \frac{4R}{3\pi}\int_0^{\pi/2} (u+iv)\, e^{-i\theta}\, d\theta \tag{23}$$

$$b_m = R^2(m-2)a_{m-2} - \frac{4R^m}{3\pi}\int_0^{\pi/2} (u+iv)\, e^{-im\theta}\, d\theta \qquad m = 3, 5, 7\ldots$$

The procedure from here follows that for the anti-plane shear problem. The contribution from A_2 to the modified potential energy functional is written in terms of the coefficients a_m and b_m which are in turn related to the displacement field along Γ_R through (23). The dominant singular solution discussed for small scale yielding is used to describe the solution on and within the small circular arc Γ_1. Its amplitude, K_ϵ, is to be found through the minimization of the modified potential energy functional. The region between Γ_1 and Γ_R is divided into a triangular grid pattern and the finite element technique is employed to connect the singular solution to the far field.

The computations for the large scale yielding problem were performed with a grid consisting of 1066 elements and an inside radius r_0 of two percent of the half crack length. The calculated values for the plastic strain intensity factor in the large scale yielding range associated with this grid are expected to be low by several per cent paralleling the findings for anti-plane shear. A check was made on the assumed condition of loading inherent in this formulation. Careful examination of the solution over the range of the loading parameter investigated here indicated that with monotonically increasing values of the load parameter, the stress invariant everywhere in the field also increased monotonically.

The results are presented in the same form as they were for the anti-plane shear problem. In the large scale yielding range, the plastic strain intensity factor is $K_\epsilon = [f(\sigma^\infty)]^n a^{n/(n+1)}$, while the formula for the plastic strain intensity factor for the small scale yielding problem is given by (7). In Fig. 6(a), $\lambda(\sigma^\infty (\equiv K_\epsilon/(K_\epsilon)_{s.s.y.}$ is plotted against $\sigma^\infty \equiv \bar{\sigma}^\infty/\bar{\sigma}_Y$. The modified formula for the crack initiation stress is

$$\sigma_i^\infty = \frac{K_{el}^c}{[\lambda(\sigma_i^\infty)]^{n+1/2n}} \cdot \frac{1}{\sqrt{\pi a}}$$

and plots of σ_i^∞/σ_Y vs. $K_{el}^c/\sigma_Y\sqrt{\pi a}$ are given in Fig. 6(b) for $n = 3$ and 9.

The elastic-plastic boundaries corresponding to the above calculations are exhibited in Fig. 7. At an applied stress level of half the yield stress the maximum extent of the

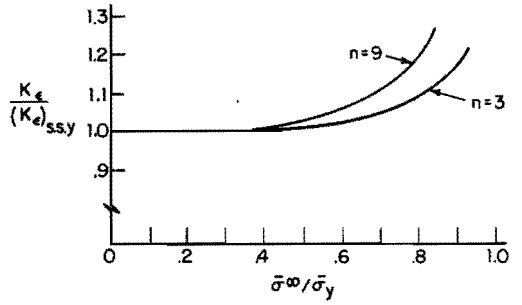

Fig. 6(a). The plastic strain intensity factor as a function of the applied stress for tensile loading.

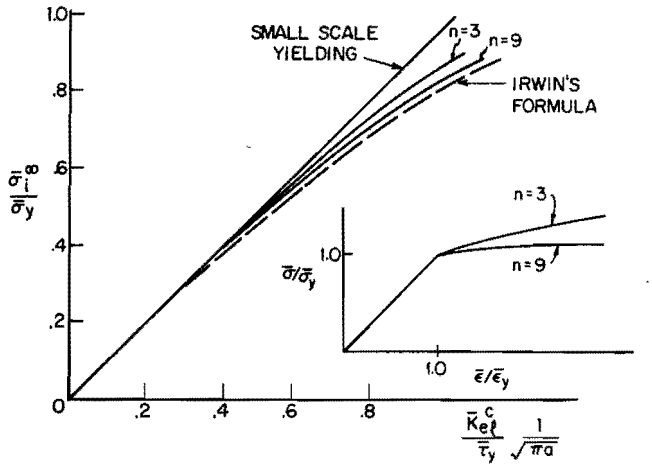

Fig. 6(b). The critical initiation stress for large scale yielding, tension.

elastic-plastic boundary is already greater than 40 per cent of the half crack length. Even so, elastic fracture mechanics, which is based on the dominant singularity of the purely elastic solution, still gives quite accurate predictions for the critical initiation stress at this level of applied stress.

The present predictions are now compared with predictions for fracture initiation based on two perfect-plasticity models. The first, due to Irwin†, is a semi-empirical adjustment of the elastic stress intensity factor to take into account the size of the plastic zone. Irwin makes use of the plastic zone size predicted for the perfect-plasticity, anti-plane shear problem and argues that the effective crack length is increased by an amount comparable to the size of the plastic zone. For the present problem, Irwin's suggestion for the modified elastic stress intensity factor is

$$\frac{K_{el}^{c}}{(1+\tfrac{1}{2}\sigma^{\infty 2})^{1/2}}$$

The predictions for the critical stress based on this are included in Fig. 6(b). Irwin's formula is quite good for low hardening materials over the range of the loading parameter plotted.

†Private communication, see also [1].

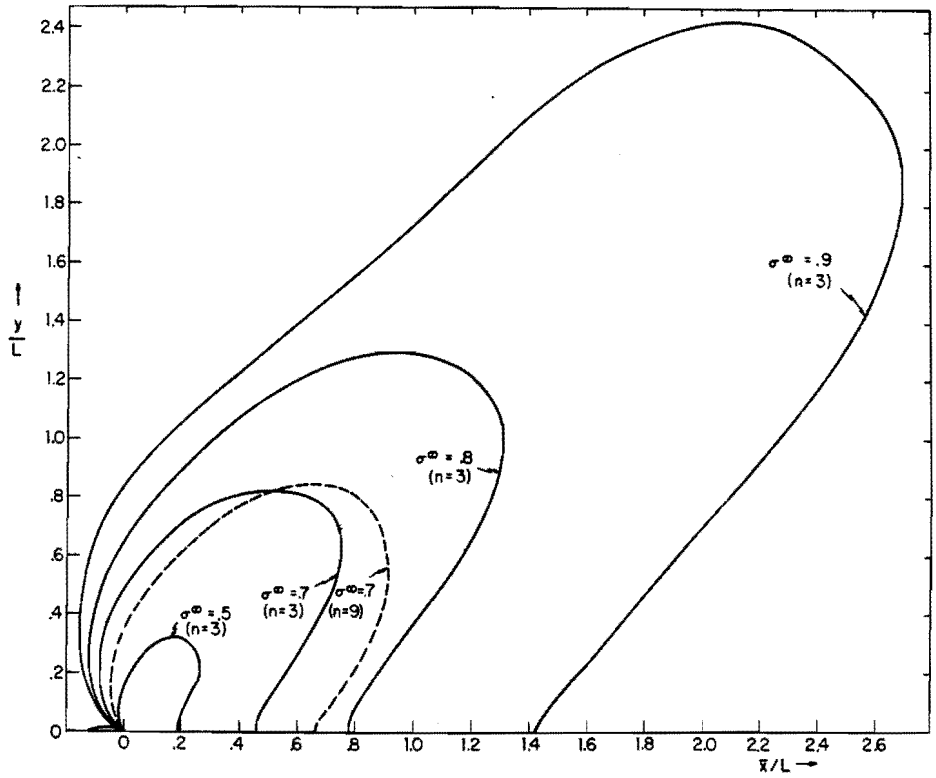

Fig. 7. Elastic-plastic boundaries for a crack subjected to a remote field. The half crack length is unity and the crack tip is taken at $\bar{x} = 0$.

The Dugdale–Barenblatt model, for the perfect-plasticity treatment of necking ahead of the crack tip in thin sheets of certain metals, is the basis of the second comparison. The crack opening displacement, the separation which occurs between the top and bottom faces of the crack at the tip, as predicted by this model [2] is

$$\delta = \frac{8a}{\pi} \bar{\epsilon}_Y \log [\sec (\sigma^\infty \frac{\pi}{2})]. \tag{24}$$

The associated fracture initiation criterion for a sequence of sheets with identical thicknesses is that the crack opening displacement reach a critical value δ^c. For small scale yielding this criterion leads to

$$\sigma_i^\infty = \sqrt{\frac{\delta^c}{\pi a}}$$

Where there is no restriction on the applied stress, the critical stress is given by (24) with δ identified with δ^c. The resulting predictions fall between the present results for $n = 9$ and those from Irwin's formula.

Rice [2, p. 293] has discussed the extension of fracture mechanics into the large scale yielding range using results from the anti-plane shear problem as well as from the

Dugdale–Barenblatt model. Instead of emphasizing the plastic intensity factors, he uses the value of a path independent integral defined for deformation theory as a measure of the level of deformation at the crack tip. It can readily be shown that these two approaches lead to identical results as long as a deformation theory of plasticity is employed. The present approach which accents the use of the plastic intensity factors is not restricted to use of a deformation theory as has been discussed and may, for this reason, be somewhat more attractive.

SUMMARY

The initial fracture predictions from classical fracture mechanics for cracked sheets in tension are quite accurate for applied stresses up to approximately half the yield stress, even though at half the yield stress the elastic-plastic boundary has been distorted considerably from that associated with the small scale yielding solution. For cracks of shorter length which fracture at higher stress levels, the critical initiation stress is found to deviate more from the small scale yielding predictions as the strain hardening capacity is reduced. Very similar conclusions follow from previous work on the anti-plane shear problem.

The method developed here for combining the knowledge of the dominant singular solution with the finite element technique to obtain accurate solutions in the neighborhood of the crack tip is also applicable to the treatment of problems involving cracks in finite bodies. It is for unusual geometries that the finite element technique is particularly attractive. The application of these techniques to the calculation of elastic stress intensity factors is straightforward and has been carried out for each of the problems considered in this study.

REFERENCES

[1] F. A. McClintock and G. R. Irwin, Plastic aspects of fracture mechanics. *ASTM Spec. Tech. Publ.* No. 381, 84 (1965).
[2] J. R. Rice, Mathematical analysis in the mechanics of fracture. *Fracture* Vol. II, pp. 191–311. Academic Press, New York, (1968).
[3] J. A. Hult and F. A. McClintock, Elastic-plastic stress and strain distribution around sharp notches under repeated shear. *Proc. 9th Int. Congr. Appl. Mech., Brussels.* Vol. 8, pp. 51–58 (1956).
[4] H. Neuber, Theory of stress concentration for shear-strain prismatical bodies with arbitrary non-linear stress strain law. *ASME* **83-E**, 544 (1961).
[5] J. R. Rice, Stresses due to a sharp notch in a work hardening elastic plastic material loaded by longtudinal shear. *J. appl. Mech.* **34**, 287–298 (1967).
[6] J. R. Rice and G. Rosengren, Plane strain deformation near a crack tip in a power-hardening material. *J. Mech. Phys. Solids* **16**, (1968).
[7] J. W. Hutchinson, Singular behavior at the end of a tensile crack in a hardening material. *J. Mech. Phys. Solids* **16**, 13 (1968).
[8] J. W. Hutchinson, Plastic stress and strain fields at a crack tip. *J. Mech. Phys. Solids* **16**, 337 (1968).
[9] P. C. Paris and G. C. Sih, Stress analysis of cracks. *ASTM Spec. Tech. Publ.* No. 381, 30 (1965).
[10] W. F. Brown and J. E. Srawley, Plane strain crack toughness testing of high strength metallic materials. *ASTM Spec. Tech. Publ.* No. 410 (1966).
[11] I. S. Tuba, private communication.
[12] G. Fix, Higher-order rayleigh-ritz approximations. *J. Math. Mech.* **18**, 645–658 (1969).
[13] O. C. Zienkiewicz, *The Finite Element Method in Structural and Continuum Mechanics.* McGraw-Hill, New York (1967).
[14] B. Budiansky, Extension of michell's theorem to problems of plasticity and creep. *Q. appl. Math.* **16** 307–309 (1958).
[15] N. I. Muskhelishvili, *Some Basic Problems of the Mathematical Theory of Elasticity.* N.V.P. Noordhoff Groningen, Holland (1963).

(*Received* 10 *May* 1969)